Electronic Supplementary Material (ESI) for Journal of Materials Chemistry A.

Supporting information

Single oxygen linear ether (SOLE) based electrolytes for fast-charging and low-temperature Li-ion batteries

Zongjian Li,[a] Jing Liu,[a] Xinying Bi [a] Yunan Qin,[a] Tao Gao[a]*

[a]Department of Chemical Engineering, University of Utah, Salt Lake City, Utah, USA 84114

*Email: taogao@chemeng.utah.edu

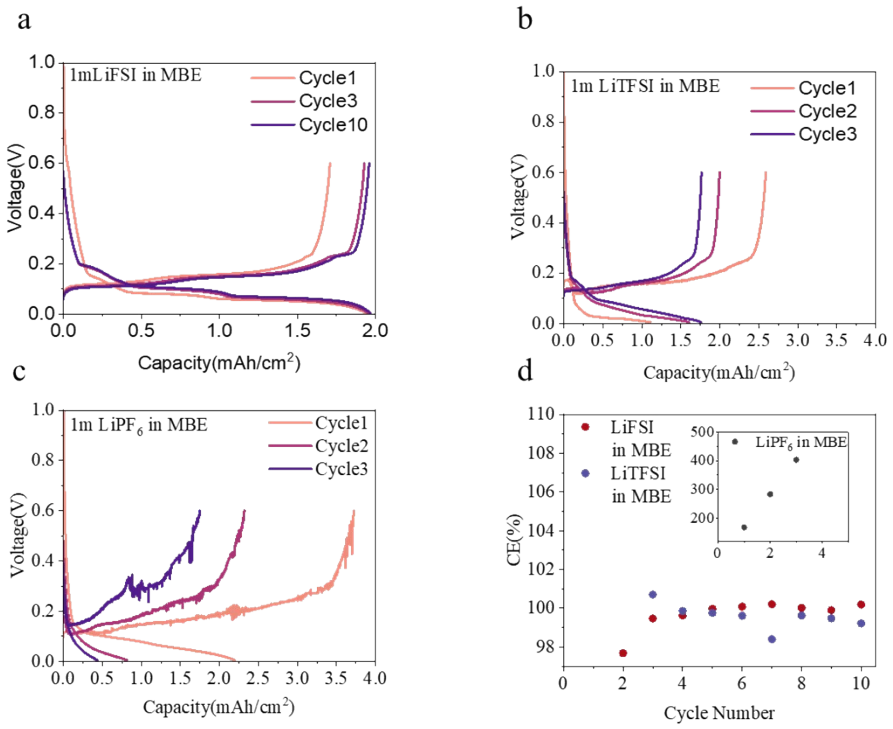

Fig. S1 Cycling performance of Li|Gr cells made by 1m (a) LiFSI; (b) LiTFSI; (c) $LiPF_6$ in MBE; (d) the CE of Li|Gr cells made by 1m LiFSI and LiTFSI in MBE. (The cell made by 1m $LiPF_6$ in MBE was broken after 3 cycles).

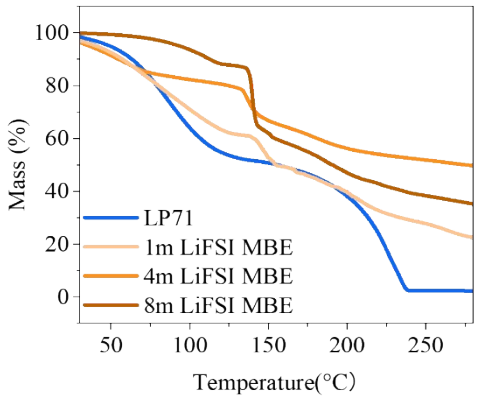

Fig. S2 TGA data of LP71 and different concentration of LiFSI in MBE solvent.

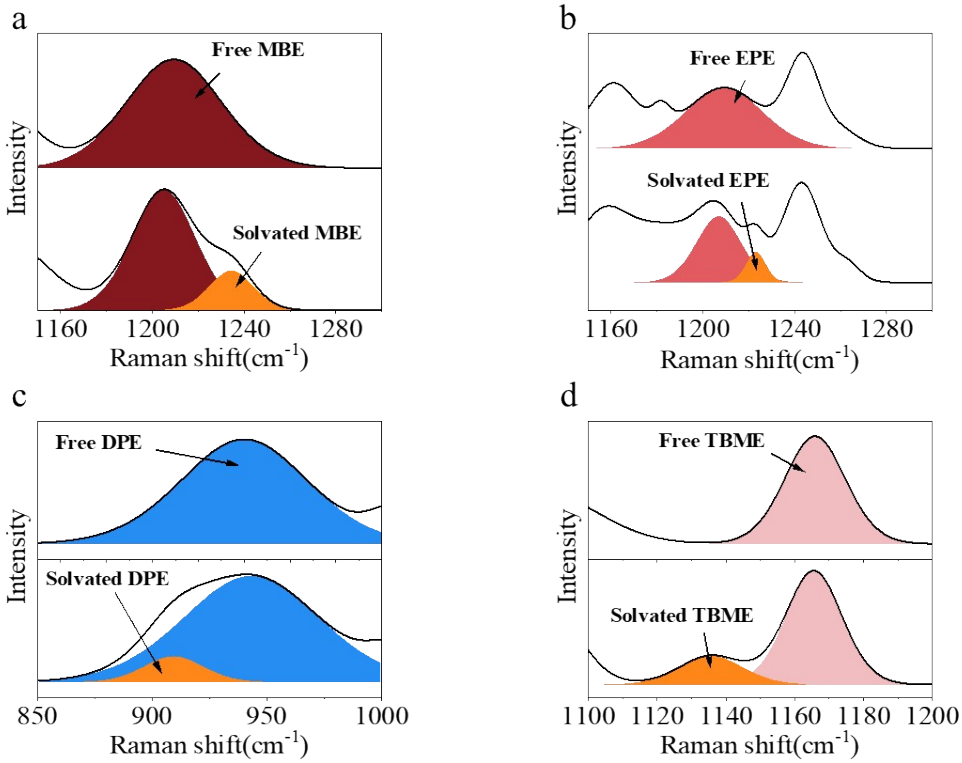

Fig. S3 Raman spectra for 1m LiFSI in (a) MBE; (b)EPE; (c) DPE; (d) TBME

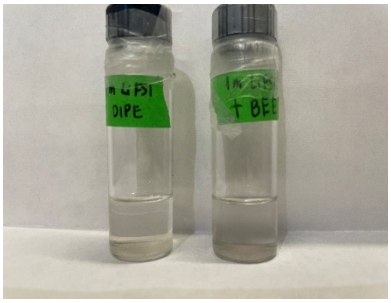

Fig. S4 Phase separation of 1m LiFSI dissolved in DIPE and TBEE (left: DIPE; right: TBEE)

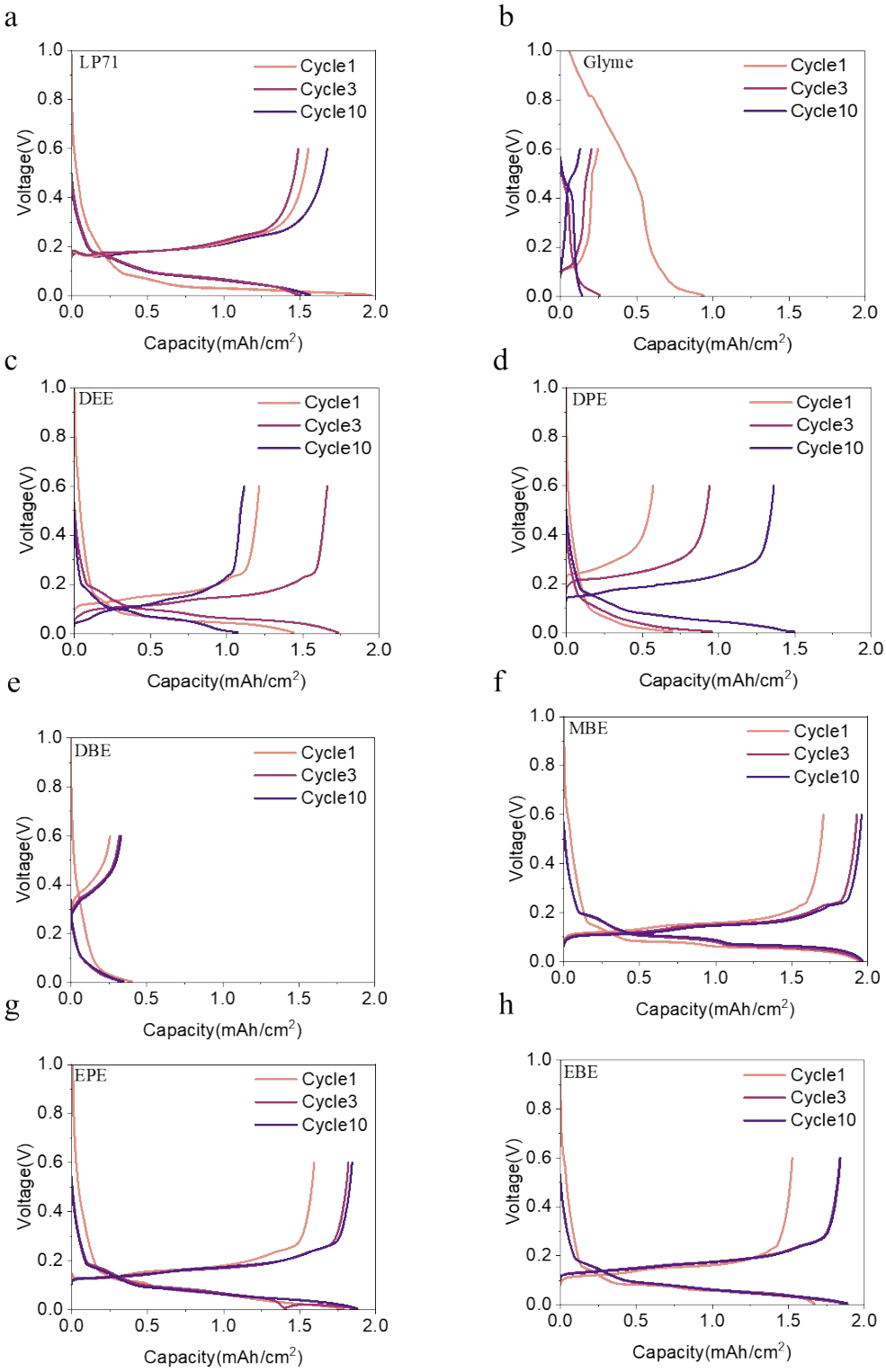

Fig. S5 Voltage profile of the 1st, 3rd, 10th cycle of Li|Gr cells with LP71, Glyme and SOLE electrolytes. (a)LP71; (b)Glyme; (c)DEE; (d)DPE; (e)DBE; (f)MBE; (g)EPE; (h)EBE

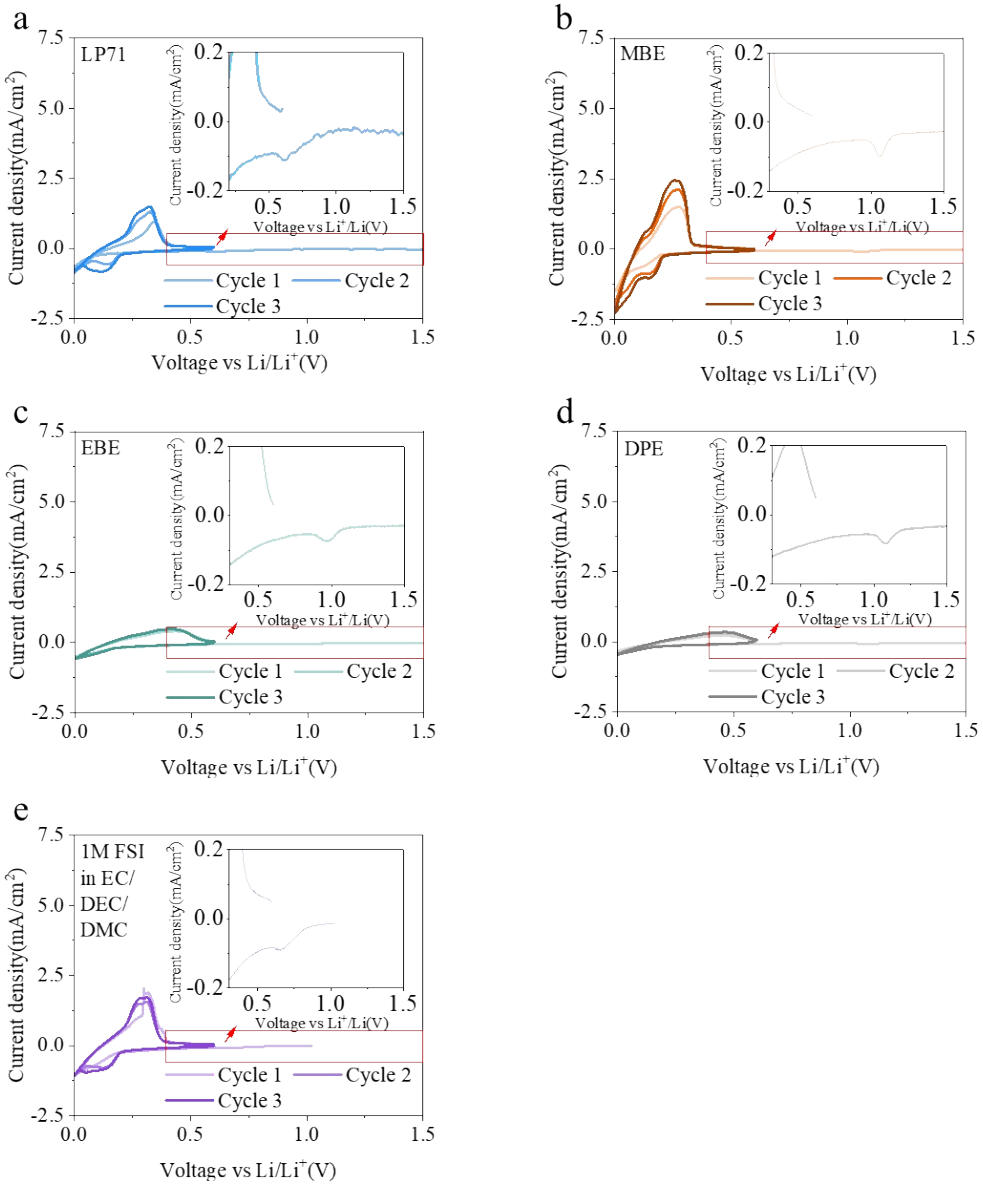

Fig. S6 Cyclic voltammetry of Li|Gr cells. (a) LP71; (b)MBE; (c) EBE; (d) DPE; (e) 1mLiFSI in EC/DEC/DMC

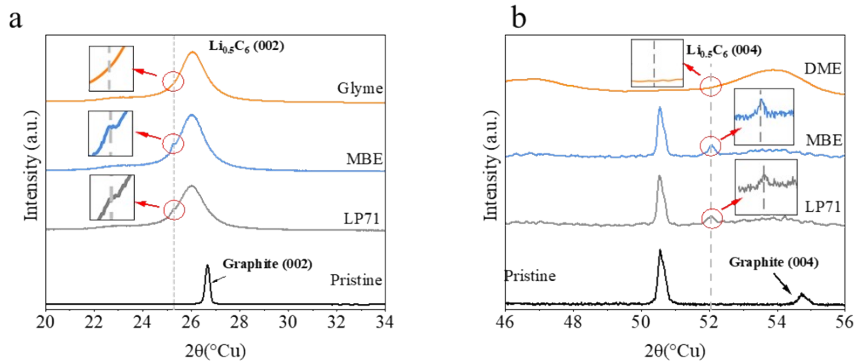

Fig. S7 XRD patterns of intercalated graphite, which is intercalated in Glyme, MBE, and LP71. The pristine graphite is set as control. The broad slope at about 26° can be attributed to no graphitic carbon fibers.[1]

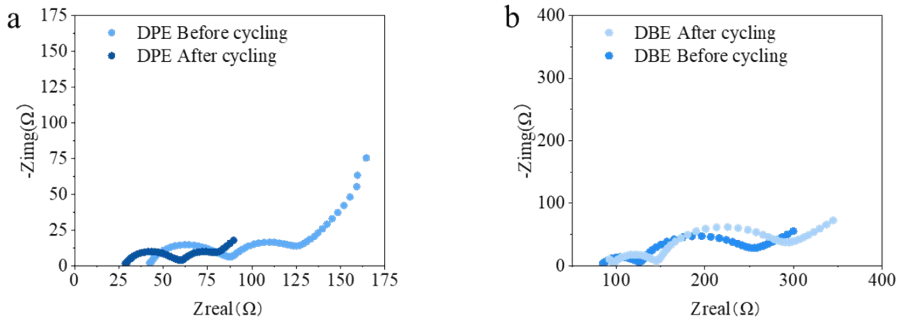

Fig. S8 EIS data for Li|Gr cells before and after 30 cycles with (a) EPE; (b) DBE

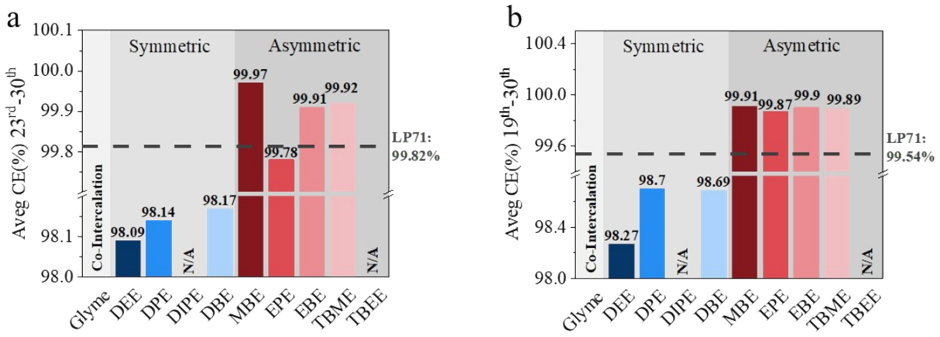

Fig. S9 The average CE of (a) last 8 cycles and (b) last 12 cycles of Li|Gr cells made by control and SOLE electrolytes and benchmark.

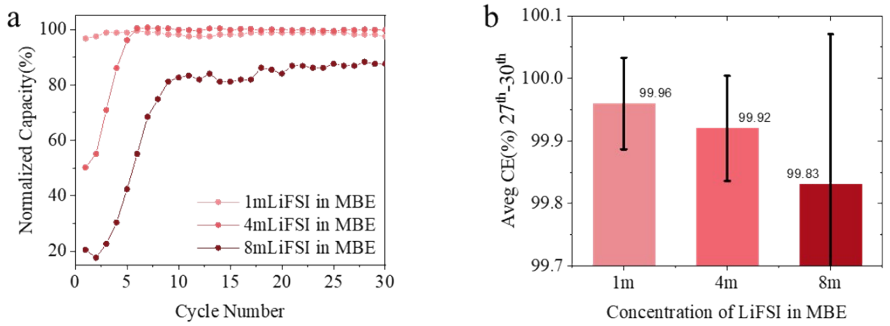

Fig. S10 (a) Cycling performance and (b) average CE of 27th- 30th cycle of Li|Gr cells with different concentration of LiFSI in MBE

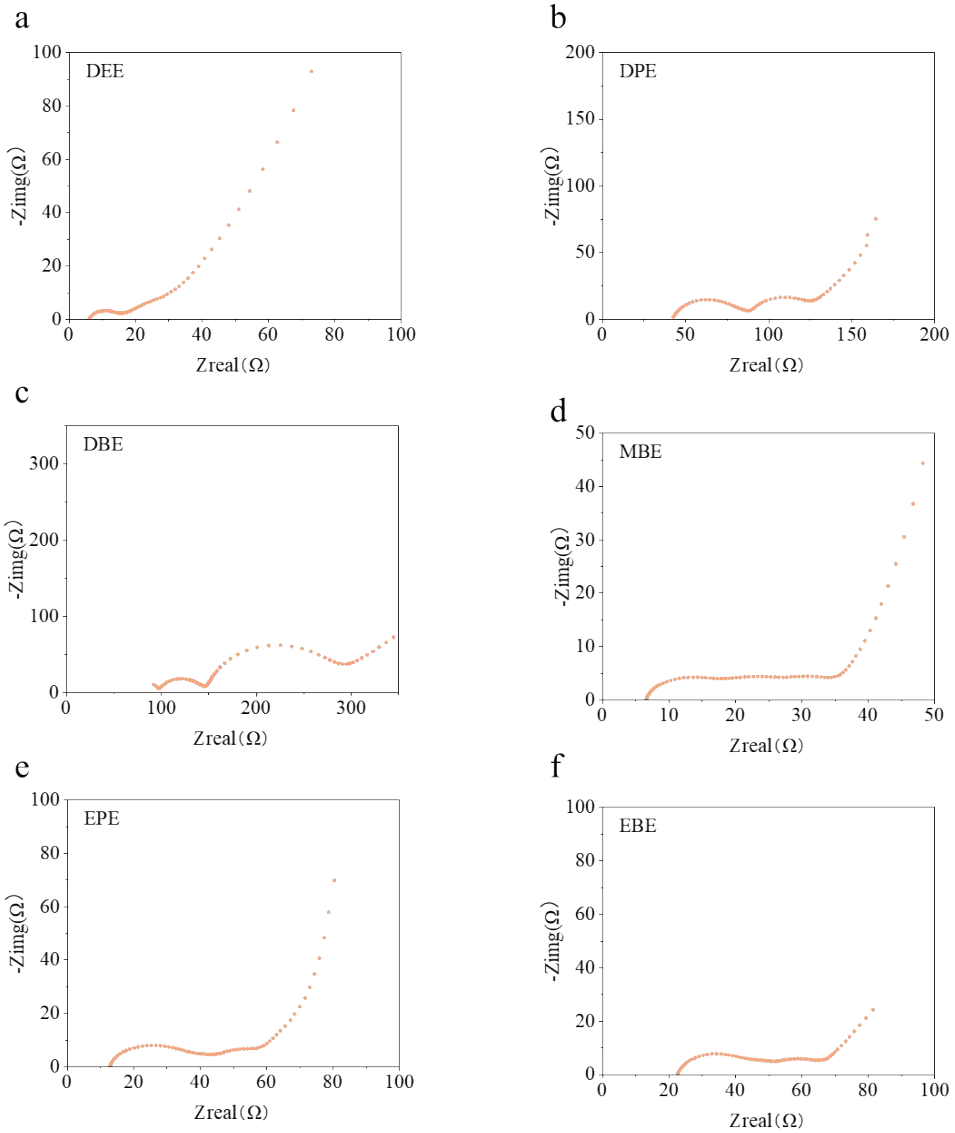

Fig. S11 EIS data of Li|Gr cells after 3 cycles' SEI formation. (a) DEE; (b)DPE; (c)DBE; (d)MBE; (e)EPE; (f)EBE

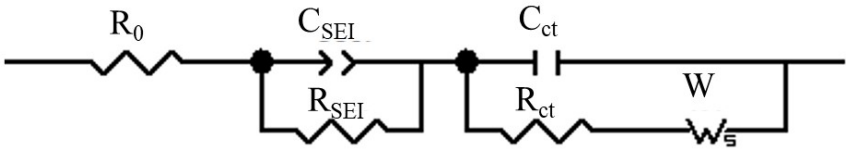

Fig. S12 Equivalent circuit model used for fitting the EIS results of Li|Gr half-cells;

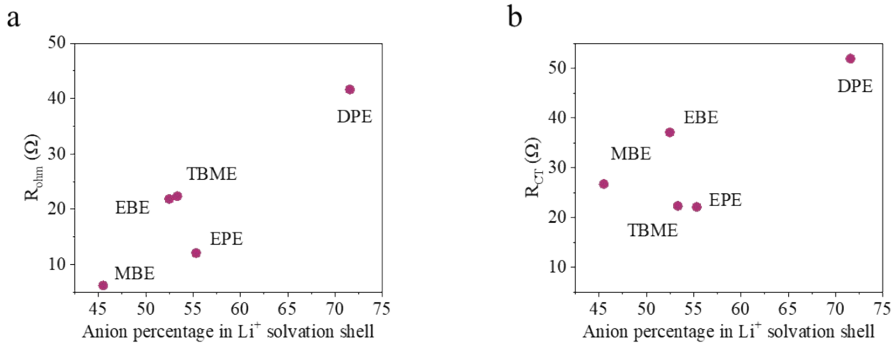

Fig. S13 The relationship between (a)R_{ohm}, (b)R_{ct} of Li|Gr cells and anion percentage in Li^+ solvation shell.

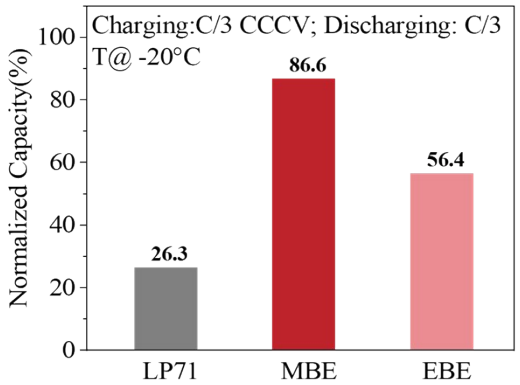

Fig. S14 Normalized capacity of Li|Gr cells at -20°C low temperature (C/3 CCCV charging, C/3 discharging).

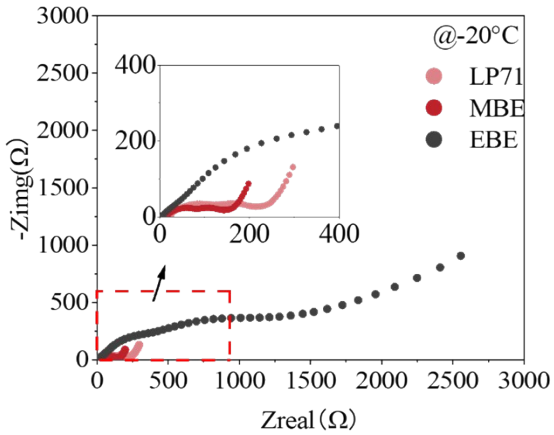

Fig. S15 EIS results of Li|Gr cells made by LP71, MBE and EBE at -20°C.

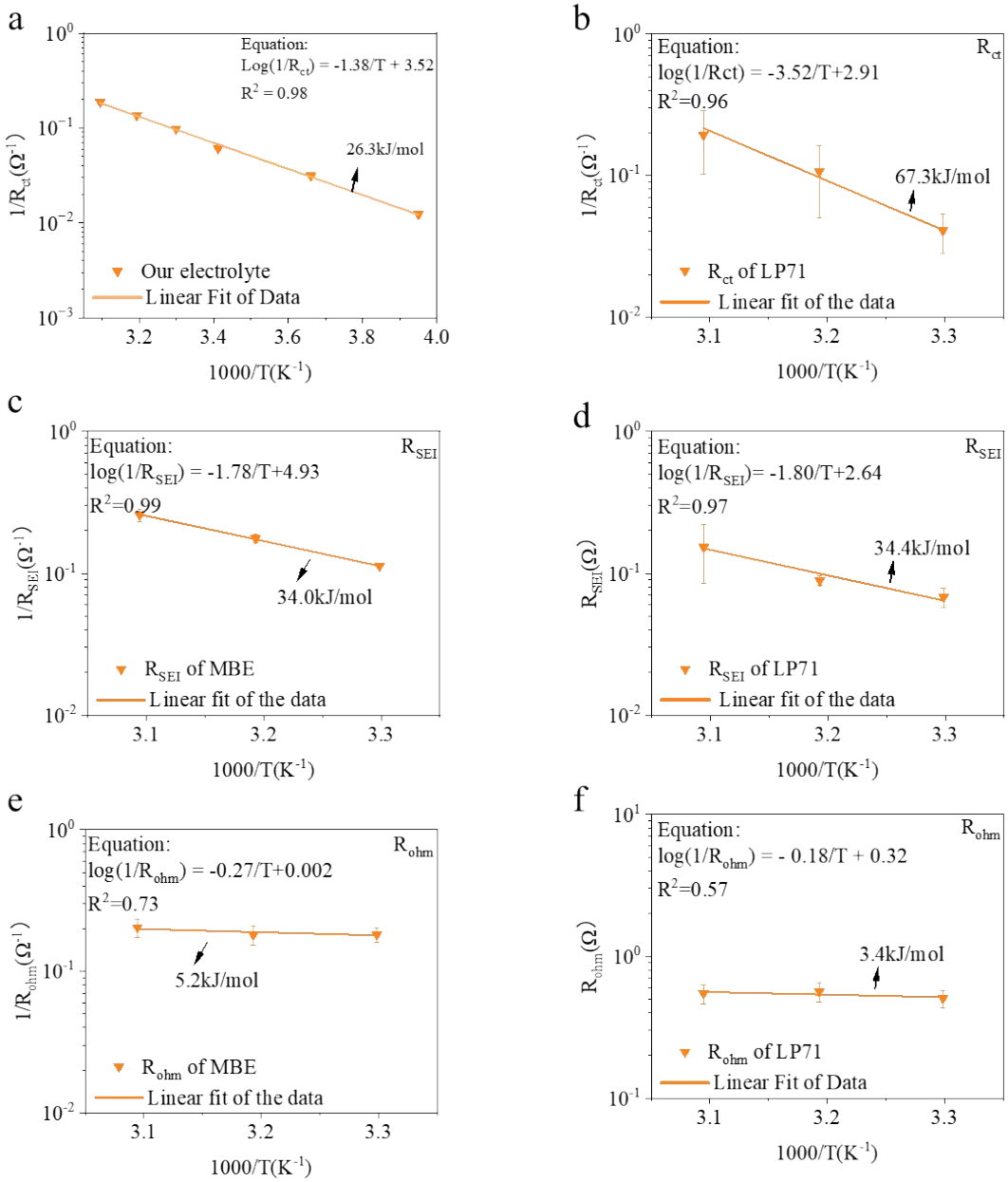

Fig. S16 The Arrhenius plot of a Li|Gr cell with a), c) and e) MBE electrolyte; b), d) and f) at the fully de-lithiated state at different temperatures.

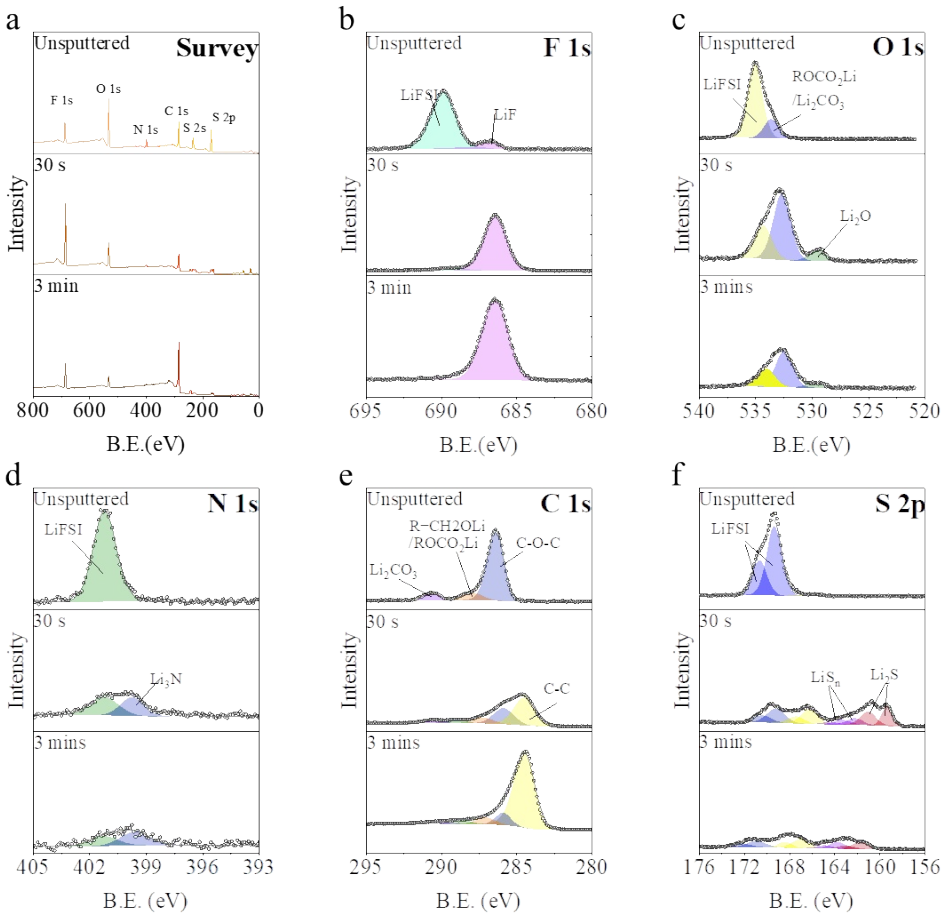

Fig. S17 XPS of the graphite electrode cycled in Li|Gr half-cell using DPE electrolyte. (a) XPS survey; (b)-(f) high-resolution XPS spectra of F 1s, O 1s, N 1s, C 1s and S 2p

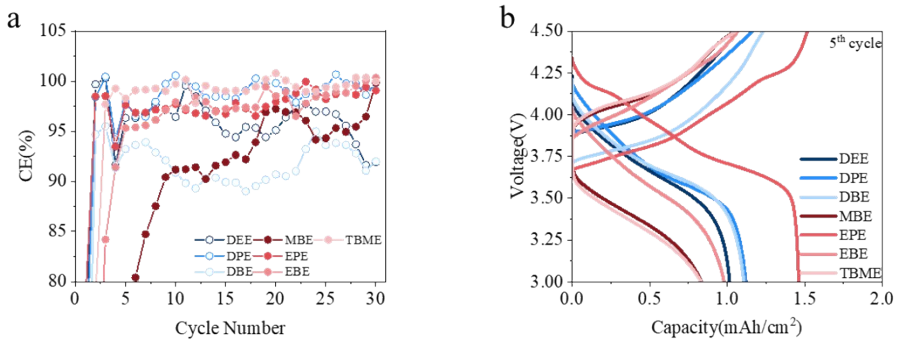

Fig. S18 Cycling performance of Gr|NMC cells made by SOLE electrolytes. (a) Coulombic Efficiency of each cell; (b) Charging and discharging profile of the 5th cycle.

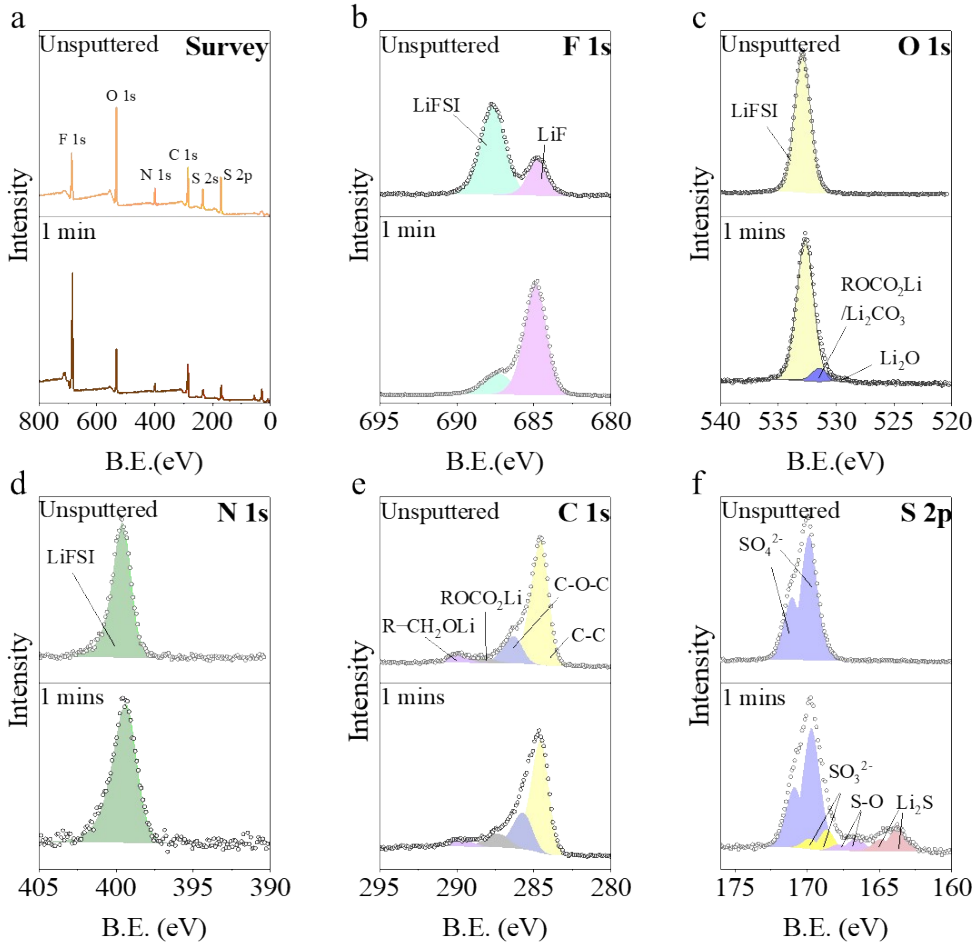

Fig. S19 XPS results of the cycled NMC electrode in MBE electrolyte. (a) XPS survey; (b)-(f) high-resolution XPS spectra of F 1s, O 1s, N 1s, C 1s and S 2p.

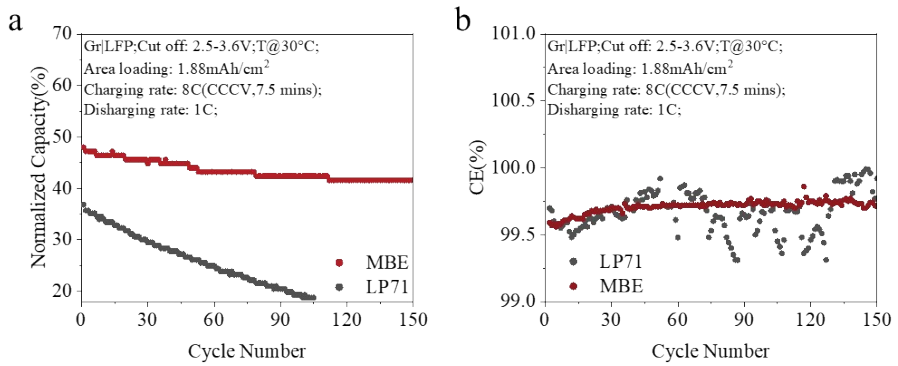

Fig. S20 Cycling performance of Gr|LFP cells made by LP71 and MBE at 8C rate. (a) capacity; (b) CE.

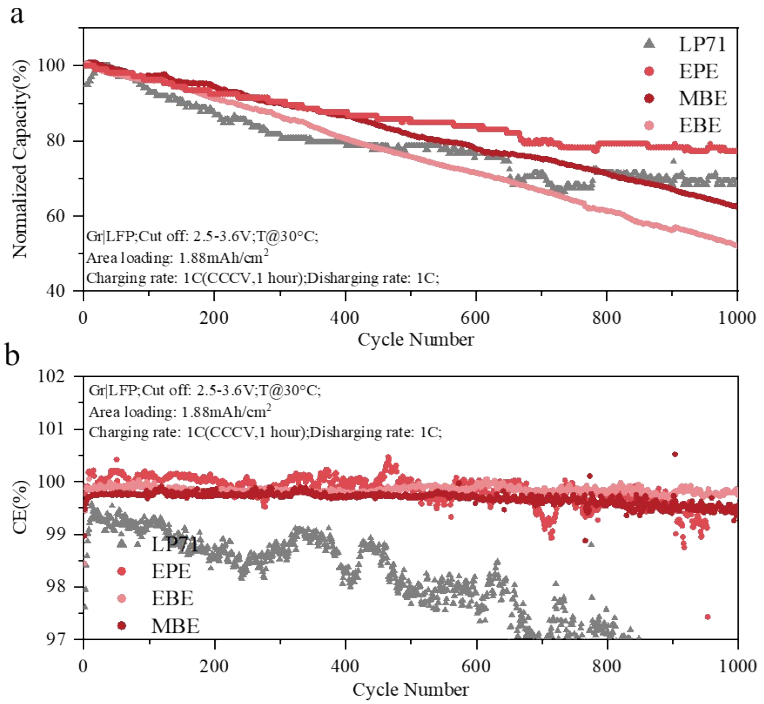

Fig. S21 Cycling performance of Gr|LFP cells at 1C rate. (a) capacity; (b) CE.

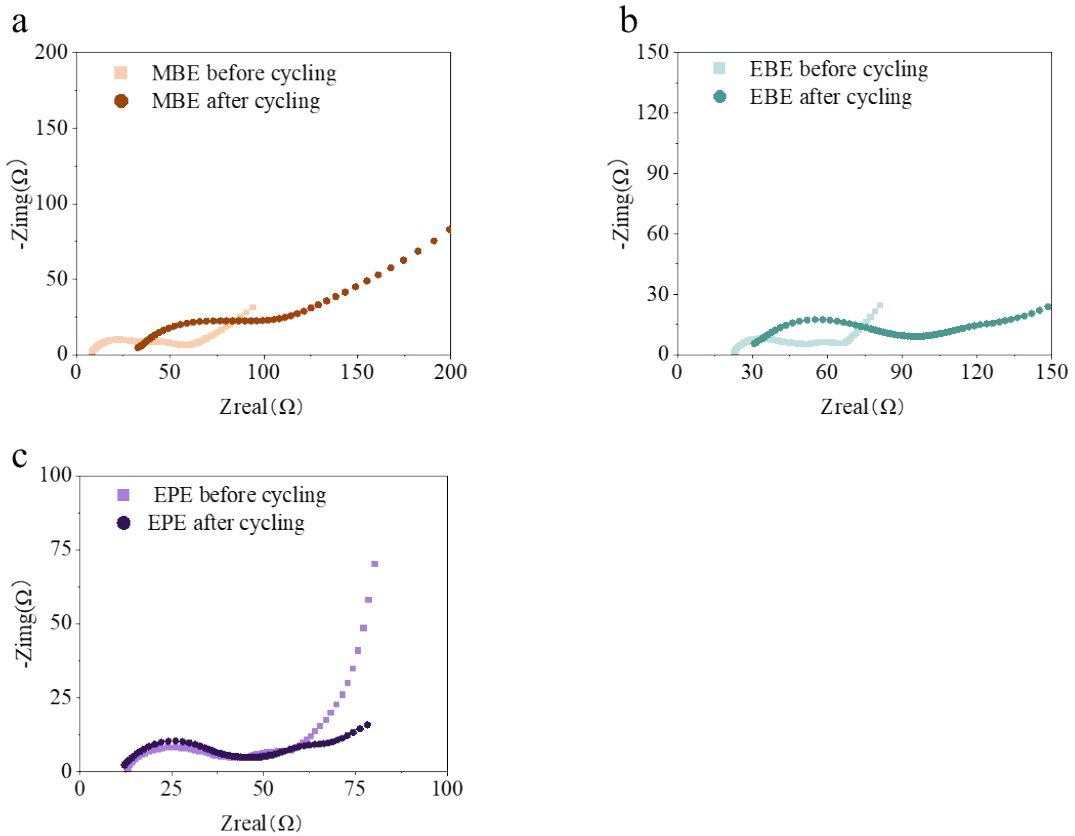

Fig. S22 The EIS results of Gr|LFP cells made by (a) MBE electrolyte, (b) EBE electrolyte and (c) EPE electrolyte before and after 1000 cycles at the fully de-lithiated state.

Table S1. Concentration of each SOLE electrolyte.

Electrolyte	DEE	DPE	DBE	MBE	EPE	EBE	TBME
Density(g/cm3)	0.713	0.736	0.768	0.744	0.739	0.750	0.740
Molality(mol/kg)	1	1	1	1	1	1	1
Molarity(mol/L)	0.71	0.69	0.70	0.74	0.72	0.69	0.70

Table S2 Structure and Viscosity of SOLE Solvents and benchmark

Category	Compound	Abb.	Structure	(Cp)	Ref.	Dielectric constant	Dipole
Control	1m $LiPF_6$ in 1/1/1 wt/wt/wt EC/DMC/DEC	LP71					
	Dimethoxyethane	Glyme	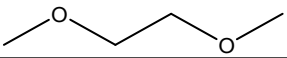	0.41 at 25 °C	2	7.3	1.7
Symmetric SOLE	Diethyl ether	DEE	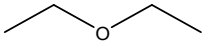	0.235 at 20°C	3	4.33	1.3
	Dipropyl ether	DPE	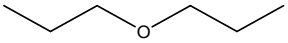			3.39	1.12
	Diisopropyl ether	DIPE	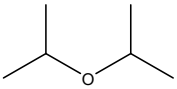	0.33 at 20°C	4	3.8	1.3
	Dibutyl ether	DBE	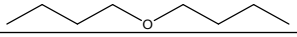	0.69 at 20°C	4	3.1	1.18
Asymmetric SOLE	Methyl Butyl ether	MBE	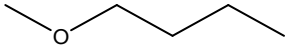			4.2	1.27
	Ethyl Propyl ether	EPE	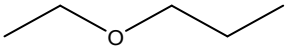				1.16
	Ethyl Butyl ether	EBE	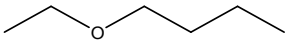				1.24
	tert-Butyl Methyl ether	TBME	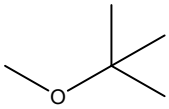	0.65 at 25°C	5	4.5	1.32
	tert-Butyl Ethyl ether	TBEE	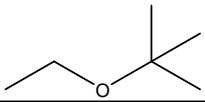	0.40 at 25°C	6		

Table S3 Solubility of some Li salts in MBE

Salt	Solubility(mol/kg)
LiFSI	8.3
LiTFSI	6.8
$LiPF_6$	3.7

Table S4 Fitting Parameters of the EIS of the Li| Gr half-cells (de-lithiated state)

Structure	Electrolyte	$R_{ohm}(\Omega)$	$R_{SEI}(\Omega)$	$R_{ct}(\Omega)$	Sum of R_{SEI} and R_{ct} (Ω)
	LP71	3.3	25.3	53.2	78.5
	DME	-	-	-	-
Symmetric solvents	DEE	6.1	7.45	19.8	27.3
	DPE	41.65	44.2	51.9	96.1
	DIPE	-	-	-	-
	DBE	92.93	56.1	145	201
Asymmetric solvents	MBE	6.195	8.21	26.7	34.9
	EPE	12.06	22.4	22.1	44.5
	EBE	21.83	18.7	37.1	55.8
	TBME	22.36	21.9	22.3	46.2
	TBEE	-	-	-	-

Table S5 Conductivity of different concentration of LiFSI in MBE

Concentration(mol/kg)	Conductivity(mS/cm)
1	0.96
2	1.2
4	1.4
6	1.2
8	0.74

Table S6 Binding Energy of Main SEI Components Reported in Literature

SEI Component	Binding Energy				
	F 1s	N 1s	S $2p_{3/2}$	C 1s	O 1s
LiFSI	687.9 [7]	400 [7]	170.3 [7]		533.2 [7]
$ROCO_2Li$				286−287 [8]	531.8 [8]
R−CH2OLi				288 [9]	
C−O−H/C−O−C				285.5 [8]	
Li_2CO_3				289.8−290.2 [8]	531.8 [8]
Li_2O					528.7 [8]
LiF	685.5 [10]				
Li_3N		397.5 [10]			
Li_2S_n (2 <n< 8)			161.7−163.2[11,12]		
Li_2S			106.5 [10]		

Table S7 Atomic Percentage of Different Elements in SEI generated by DPE.

Sputtering time	Element				
	F	O	N	S	C
Unsputtered	9.3	28.2	6.9	15.0	40.6
30s	28.8	20.2	2.9	9.8	38.2
1 min	20.0	14.9	1.9	7.9	55.2
3 mins	9.4	8.0	1.1	4.7	76.8

Table S8 Fitting Parameters of the EIS of the Gr|LFP full cells (de-lithiated state)

Electrolyte		$R_{ohm}(\Omega)$	$R_{SEI}(\Omega)$	$R_{ct}(\Omega)$	Sum of R_{SEI} and R_{ct} (Ω)
MBE	Before	7.09	17.5	47.3	64.8
	After	29.1	22.7	46.6	69.3
EBE	Before	20.7	18.67	37.1	55.77
	After	22.8	75.4	42.5	117.9
EPE	Before	12.06	22.4	23.9	46.3
	After	8.8	24.6	26.1	50.7

Reference:

1 A. Bhargav, M. Wu and Y. Fu, *J Electrochem Soc*, 2016, **163**, A1543–A1549.

2 J. Barthel, R. Neueder and H. Roch, *J Chem Eng Data*, 2000, **45**, 1007–1011.

3 X. Meng, P. Zheng, J. Wu and Z. Liu, *Fluid Phase Equilib*, 2008, **271**, 1–5.

4 X. Meng, J. Wu and Z. Liu, *J Chem Eng Data*, 2009, **54**, 2353–2358.

5 S. Viswanathan, M. Anand Rao and D. H. L. Prasad, *J Chem Eng Data*, 2000, **45**, 764–770.

6 D. Li, X. Qin, W. Fang, M. Guo, H. Wang and Y. Feng, *Exp Therm Fluid Sci*, 2013, **48**, 163–168.

7 B. Philippe, R. Dedryveìre, M. Gorgoi, H. Rensmo, D. Gonbeau and K. Edström, *J Am Chem Soc*, 2013, **135**, 9829–9842.

8 V. Eshkenazi, E. Peled, L. Burstein and D. Golodnitsky, *Solid State Ion*, 2004, **170**, 83–91.

9 G. G. Eshetu, T. Diemant, S. Grugeon, R. J. Behm, S. Laruelle, M. Armand and S. Passerini, , DOI:10.1021/acsami.6b04406.

10 C. Xu, B. Sun, T. Gustafsson, K. Edström, D. Brandell and M. Hahlin, *J Mater Chem A Mater*, 2014, **2**, 7256–7264.

11 T. Momma, Y. Wu, H. Mikuriya, H. Nara and T. Osaka, *J Power Sources*, 2019, **430**, 228–232.

12 Y. Fu, C. Zu and A. Manthiram, *J Am Chem Soc*, 2013, **135**, 18044–18047.